Bilayers of Monomeric and Polymeric 4,*N*-POMECY and Dimyristoylphosphatidylcholine

D. A. Pink,*,† B. E. Quinn,† K. Baskin,† and E. Sackmann‡

Department of Physics, St. Francis Xavier University, P.O. Box 5000, Antigonish, Nova Scotia, Canada B2G 2W5, and Physik Department, Technische Universität München, 85748 Garching bei München, Germany

Received March 28, 1994; Revised Manuscript Received October 19, 1994®

ABSTRACT: We have modeled mixed bilayers of dimyristoylphosphatidylcholine (DMPC) and the polymerizable amphiphile 4,*N*-POMECY monomers as well as bilayers of DMPC and 4,16-POMECY polymers (macrolipids). Our intention was to answer three questions: (i) Why, with two C-16 hydrocarbon chains, does pure monomeric 4,16-POMECY exhibit a phase transition at $T_m^{up} \simeq 29$ °C? (ii) Why then do the pure (polymerized) 4,16-POMECY macrolipids possess $T_m^{p} \approx 45$ °C? (iii) What does the measured phase diagram imply about macrolipid structure. Using analytic methods and computer simulation to obtain phase diagrams, we conclude that the answer to (i) is that the entropy of the relatively long polar group contributes to reducing T_m from ~41 to ~29 °C. When the macrolipids are formed, via polymerization in their polar groups, this entropy is lost and T_m is then determined by the interaction between hydrocarbon chains which yields $T_m \approx 41$ °C. We modeled the macrolipids as (a) flexible chains, (b) compact hexagons, or (c) rigid rods of fixed length. We found that none of these models described the experimental data. We simulated the polymerization process in the bilayer and found that the average length of the polymers formed increased with initial monomer concentration. Using these results we constructed a phase diagram using model b and found good agreement with experiment. We deduced that 4,16-POMECY macrolipids formed in a bilayer are probably rigid with compact segments connected, possibly by rigid rods. We make predictions of the transition temperatures of monomeric and polymeric 4,*N*-POMECY for $N = 14$ and 18.

Introduction

The amphiphile *M*,*N*-POMECY[1] possesses two hydrocarbon chains and a head group and has the structural form

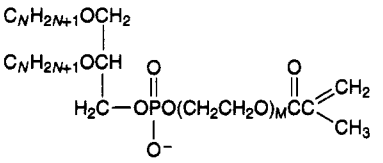

It carries one functional group attached to its head group, via a spacer $(CH_2CH_2O)_M$. These amphiphiles ("monomers") can be incorporated into giant vesicles or into supported lipid bilayers and, subsequently, photochemically polymerized in the head group via UV radiation, thereby forming linear macromolecules ("macrolipids").[2] In this way studies were carried out, using static light-scattering techniques,[3] to determine the phase diagram of vesicles containing a binary mixture of dimyristoylphosphatidylcholine (DMPC) and 4,16-POMECY.[2] The phase diagram for monomeric 4,16-POMECY showed a narrow cigarlike (two-phase region, indicating a nearly ideal mixture, extending from $T \approx$ 24 °C (pure DMPC) to $T \approx 29$ °C (pure 4,16-POMECY). For the macrolipid, only the liquidus line was determined and this increased steeply with increasing concentration below ~40% of the amphiphile, followed by a nearly-horizontal line at higher concentrations at $T \approx 45$ °C.

Three questions arise here: (i) Why is it that, with a pair of C-16 hydrocarbon chains, the "main" phase transition of the pure monomeric amphiphile occurs at ~29 °C, some 12 °C lower than the corresponding transition in bilayers of pure dipalmitoylphosphatidylcholine (DPPC) which occurs at $T \approx 41$ °C? (ii) Why then does the corresponding phase transition of the pure macrolipids occur at $T \approx 45$ °C? (iii) What can be said about the conformations and flexibility of POMECY macrolipids? It is the intention of this paper to show that the answers to i and ii might be due to the coupling of the hydrocarbon chain states to the states of the head-group polymer. To obtain an answer to iii, we shall do two things: We shall present the results of calculations of a DMPC−POMECY phase diagram and compare it to measurements carried out on this system. Then, we shall simulate the polymerization process and show the dependence of the degree of polymerization upon monomer concentration. In the next section, we shall outline the theoretical model used for the calculations and show how the polymerization of the head groups can effectively decouple them from the hydrocarbon chains. Then, we shall show the results of computer simulation for mixed bilayers of DMPC and macrolipids of fixed lengths and, finally, present results for a model of the polymerization process itself.

Theory

Pure POMECY System. We use a model that has been used to study the hydrocarbon chain main phase transition and which has successfully accounted for the temperature dependence of Raman intensities and the numbers of gauche bonds per hydrocarbon chain in phosphatidylcholines (PC) for $T < T_m$, the main lipid bilayer phase transition temperature.[4−6] It assigns an internal energy E_n (arising from gauche isomers) to the nth molecular state, together with a degeneracy (number of such states possessing energy E_n), D_n, and a molecular cross-section area projected onto the local plane of the bilayer, A_n. It assumes that there exists an interaction energy $-J_0 J_{nm}$ between two nearest-

† St. Francis Xavier University.
‡ Technische Universität München.
® Abstract published in *Advance ACS Abstracts,* January 1, 1995.

0024-9297/95/2228-0736$09.00/0

neighbor molecules in states n and m, respectively. The Hamiltonian operator for such a model is

$$\mathscr{H} = \frac{-J_0}{2}\sum_{\langle ij\rangle}\sum_{nm} J_{nm}\mathscr{L}_{in}\mathscr{L}_{jm} + \sum_i\sum_n \epsilon_n \mathscr{L}_{in} \qquad (1)$$

$$\epsilon_n = E_n + \Pi A_n$$

where $\mathscr{L}_{in}$ is a projection operator for the ith lipid in state n, ϵ_n is the energy of a single isolated molecule, and $\langle ij\rangle$ indicates a sum over nearest-neighbor pairs of lipids i and j. Here, Π is an effective lateral pressure, due to the water-mediated interactions in the polar region, acting on the hydrocarbon chains and the polar group polymers, which gives rise to the pressure–area term in (1). We define an operator, $\mathscr{F}$, which includes the degeneracies

$$\mathscr{F} = \mathscr{H} - k_B T\sum_i\sum_n ln(D_n)\mathscr{L}_{in} \qquad (2)$$

A simple model suffices to show how the phase transition comes about, in general, and what the effect is of the polar group. We assume that each molecule possesses only two states: a ground state, g, possessing E_g, $A_g \approx 42$ Å^2, and D_g, in which the hydrocarbon chains are essentially extended, and an excited state, e, possessing $E_e > E_g$, $A_e \approx 65$ Å$^2 > A_g$, and $D_e \gg D_g$. Note that the degeneracies of the polar region are included in D_g and D_e and that, when the molecules are in their ground state, sufficiently long polar group polymers will be essentially extended. If we use the transformation[7,8]

$$\mathscr{L}_{ig} = {}^1/_2(1 + \sigma_i), \quad \mathscr{L}_{ie} = {}^1/_2(1 - \sigma_i), \quad \sigma_i = \pm 1 \qquad (3)$$

then we obtain

$$\mathscr{F} = -E_0 - \frac{J}{2}\sum_{\langle ij\rangle}\sigma_i\sigma_j - H\sum_i \sigma_i$$

$$J = \frac{J_0}{4}(J_{gg} - 2J_{ge} + J_{ee}) \qquad (4)$$

$$H = \frac{J_0}{4}z(J_{gg} - J_{ee}) + {}^1/_2[E_e - E_g + \Pi(A_e - A_g) - k_B T\, ln(D_e/D_g)]$$

where z is the effective number of nearest neighbors. A discontinuous phase transition occurs at T_m, given by

$$T_m = \frac{J_0}{2}z\frac{(J_{gg} - J_{ee}) + (E_e - E_g) + \Pi(A_e - A_g)}{k_B\, ln(D_e/D_g)} \qquad (5)$$

if $T_m < T^*$, the critical temperature of the system described by (4) when the term involving H is ignored.

For a given length of hydrocarbon chain (N) and polymer polar group (M), when the lipids are unpolymerized, J_{nm} and E_n increase as the first or second power of $M + N$, the A_n values are essentially independent of these lengths, and D_n increases like λ^{M+N}. This is a consequence of the molecules being sufficiently closely packed so as to form a bilayer membrane. Such packing essentially eliminates hydrocarbon chain configurations which "bend back" upon themselves. When the lipids are polymerized at the end of their polar groups, as in 4,16-POMECY, it is plausible that D_n increases like λ^N but is essentially independent of M. The reason is that the polar group polymer has been made more immobile by the removal of the degree of freedom previously associated with its free end. If we write

$$D_e = D_{ce}D_{pe} \qquad D_g = D_{cg}D_{pg} \qquad (6)$$

where $D_{c\alpha}$ and $D_{p\alpha}$ are the degeneracies of the hydrocarbon chains and polar groups when the molecule is in state α, then

$$T_M^{up} \simeq \frac{T_m^0}{\left[1 + \dfrac{ln(D_{pe}/D_{pg})}{ln(D_{ce}/D_{cg})}\right]} + \frac{E_{pe} - E_{pg} + \Delta\Pi(A_e - A_g)}{k_B\, ln\left(\dfrac{D_{ce}}{D_{cg}}\dfrac{D_{pe}}{D_{pg}}\right)} \qquad (7)$$

where the superscript "up" denotes unpolymerized, T_m^0 is the corresponding transition temperature for the same hydrocarbon chains and a PC polar group, and $\Delta\Pi$ is the difference in the effective lateral pressure between C-16 hydrocarbon chains in a POMECY molecule and a lipid molecule with a PC polar group.

When the polar groups are polymerized and, therefore, tethered at both ends, the removal of the extra degree of freedom associated with the polar group polymer will result in $D_{pe} \approx D_{pg}$, $E_{pe} \approx E_{pg}$, so that

$$T_m^p \simeq T_m^0 + \frac{\Delta\Pi(A_e - A_g)}{k_B\, ln\left(\dfrac{D_{ce}}{D_{cg}}\right)} \qquad (8)$$

where the superscript p indicates polymerized.

In the case that the polymerizable lipids are 4,16-POMECY, the measurements of Eggl et al. give a value for $T_m^p \simeq 318$ K (~45 °C). Using that $A_e \simeq 68$ Å^2 and that $A_g \simeq 43$ Å^2 for a molecule and that $ln(D_{ce}/D_{cg}) \simeq 18.8$ (e.g., ref 4; note that the degeneracies given there are per lipid chain, whereas here we need degeneracies per molecule) with $T_m^0 \simeq 314.2$ K (41 °C), then, if we choose $\Delta\Pi = 4$ dyn/cm, we obtain

$$T_m^p(4,16) \simeq 318\ \text{K} = 44.8\ ^\circ\text{C} \qquad (9)$$

Since this model used $\Pi = 30$ dyn/cm, this result suggests that the effective lateral pressure inside an unpolymerized 4,16-POMECY membrane is ~34 dyn/cm. In order to calculate T_m^{up}, we need to be able to estimate D_{pe}/D_{pg}. To do so, we can note that the length of the polar group is equivalent to a C-14 hydrocarbon chain. From previous calculations for excited and ground states[4] these degeneracies are about 3.54×10^4 and 15 per chain, and the energies are $\sim 1.94 \times 10^{-13}$ and $\sim 0.4 \times 10^{-13}$ erg/chain. Substituting these values into (7), we obtain $T_m^{up}(4,16) \simeq 277.3$ K in comparison to the measured value of ~302 K. We could argue, however, that D_{pe} and D_{pg} are larger than those of a C-14 chain because the cross-sectional area available to them is twice as large as for a single C-14 chain. If we assume that $D_{pe} \simeq 4 \times 10^4$ and $D_{pg} \simeq 4 \times 10^2$, then we obtain

$$T_m^{up}(4,16) \simeq 303.2\ \text{K} = 30.0\ ^\circ\text{C} \qquad (10)$$

which agrees with the experimental results. Thus, by choosing $\Delta\Pi$ from a knowledge of the experimental value of T_m^p, we see that reasonable values of polar

group degeneracies give the observed value of T_m^{up}. Using these results, we can now try to predict the transition temperatures for other cases.

(i) 4,14-POMECY. In this case $D_{ce} \approx 125 \times 10^7$ and $D_{cg} \approx 100$,[4] giving $ln(D_{ce}/D_{cg}) \approx 16.3$. Again we use $E_{pe} \simeq 1.94 \times 10^{-13}$ and $E_{pg} \simeq 0.40 \times 10^{-13}$ erg/chain for the unpolymerized case with $A_e \simeq 68$ Å^2 and $A_g \simeq 43$ Å^2. Using the values that we chose for D_{pe} ($\simeq 4 \times 10^4$) and D_{pg} ($\simeq 4 \times 10^2$) for the unpolymerized case together with $\Delta\Pi \simeq 4$ dyn/cm, we find that

$$T_m^{up}(4,14) \simeq 14.7\ ^\circ\text{C} \qquad (11)$$

$$T_m^{p}(4,14) \simeq 27.5\ ^\circ\text{C}$$

(ii) 4,18-POMECY. For this case $D_{ce} \simeq 10.2 \times 10^{12}$ and $D_{cg} \simeq 11.0 \times 10^2$, giving $ln(D_{ce}/D_{cg}) \approx 23.0$, and $E_{ce} \simeq 7.24 \times 10^{-13}$ and $E_{cg} \simeq 1.09 \times 10^{-13}$ erg/chain.[4] Again choosing the values for E_{pe}, E_{pg}, D_{pe}, and D_{pg} used above for the unpolymerized case, we predict that

$$T_m^{up}(4,18) \simeq 44.1\ ^\circ\text{C} \qquad (12)$$

$$T_m^{p}(4,18) \simeq 59.2\ ^\circ\text{C}$$

Mixed Polymerized POMECY–DMPC Systems. We represent the plane of one sheet of a bilayer by a triangular lattice, each site of which can be occupied either by a DMPC molecule or a POMECY monomer possibly belonging to a macrolipid. The Hamiltonian operator for this system is a generalization of (1),

$$\mathcal{H} = -\frac{J_0}{2}\sum_{\alpha\beta}\sum_{\langle ij\rangle}\sum_{nm} J_{nm}^{\alpha\beta}\mathcal{L}_{in}^{\alpha}\mathcal{L}_{jm}^{\beta} + \sum_{\alpha}\sum_{i}\sum_{n}\epsilon_n^{\alpha}\mathcal{L}_{in}^{\alpha} \qquad (13)$$

$$\epsilon_n^{\alpha} = E_n^{\alpha} + \Pi A_n^{\alpha}$$

where, in comparison to the symbols in (1), α and β sum over M and P, representing DMPC and 4,16-POMECY molecules, respectively. Thus, $-J_0 J_{nm}^{PM}$ is the interaction energy between nearest-neighbor molecules, one of which is DMPC in its mth state and the other POMECY in its nth state. For simplicity we have put the effective pressure, Π, to be independent of the environment, and choose it to be 30 dyn/cm (above). The operator, $\mathcal{F}$, which now refers to molecular states and which ignores the configurational entropy of mixing, is

$$\mathcal{F} = \mathcal{H} - k_B T\sum_{\alpha}\sum_{i}\sum_{n} ln(D_n^{\alpha})\mathcal{L}_{in}^{\alpha} \qquad (14)$$

The hydrocarbon chain states of DMPC are those used before,[9] while we used the corresponding states for a C-16 chain[9] to model the hydrocarbon chain states of polymeric 4,16-POMECY. In accord with the argument of the previous section, we did not assign internal states to the polymeric POMECY polar groups. The choice of 30 dyn/cm for Π means that, as the macrolipid concentration approaches unity, a phase transition will be observed at ~41 °C instead of ~45 °C. We feel that, since we believe that we understand the basis of this small difference, it is unnecessary to complicate the theoretical models in this section. Instead, our goal is to try to understand the properties of the phase diagram reported by Eggl et al.[2]

We studied the thermodynamics of this system using Monte Carlo (MC) computer simulation techniques, making use of the Metropolis algorithm.[9,10] In each MC step we attempted to change the state of each DMPC molecule and each POMECY monomer. We also attempted to move either each POMECY monomer or each POMECY macrolipid depending upon which macrolipid model we are using. In attempting changes the Metropolis algorithm was used in all procedures. This algorithm involves using $\mathcal{F}$ to calculate the energy of the system, (14), both before the change is attempted and after the change has taken place. Let these energies be f_1 and f_2. Define $\Delta f = f_2 - f_1$. Then, if $\Delta f < 0$, the change is permitted. If $\Delta f > 0$, then a random number, R, where $0 \le R < 1$, is selected, and if $R \le \exp(-\Delta f/k_B T)$, then the change is permitted. Otherwise, the change is not permitted. We next describe the macrolipid models used.

Models of POMECY Macrolipids. Since one of the goals of this paper was to deduce information on the flexibility of POMECY macrolipids, we considered three extreme models: (i) Model I, in which a macrolipid is a flexible self-avoiding polymer, constrained to move in two dimensions. In this case, in each MC step, we attempted to move each POMECY monomer, to a randomly chosen nearest-neighbor site, using the bond-stretching algorithm of Carmesin and Kremer.[11] The move is attempted only if the site chosen is occupied by a DMPC molecule. Bonds were permitted to stretch so that consecutive monomers in a macrolipid may occupy second neighbor sites (e.g., ref 12, Figure 2A), but bond-crossing was not permitted. (ii) Model II, in which the macrolipid was assumed to be rigid and compact. Here a macrolipid was represented by a hexagon, each site of which was occupied by a monomer. At each MC step one of the six symmetry directions was chosen and, if in translating the hexagon by one lattice constant, POMECY monomers would occupy sites occupied only by DMPC molecules, then the move was attempted. If the move was permitted, then the DMPC molecules so displaced were moved to the sites vacated by the POMECY monomers of the macrolipids (see, e.g., ref 9). In addition to translations, an attempt was also made to rotate each hexagon by angles $\pm\pi/3$ at each MC step. (iii) Model III, in which a POMECY macrolipid was assumed to be a rigid rod, one monomer in width. The method and criteria for moving it were the same as for model II. No attempt was made to rotate the rod. Models II and III and their movement are shown in Figure 1.

Polymerization of POMECY Monomers. We assumed that this process took place in a homogeneous phase for temperatures sufficiently higher than the transition temperatures of both lipids, so that we can assume that essentially all hydrocarbon chains are in their excited states. We represented the plane of the bilayer by a triangular lattice of N^2 sites and randomly distributed xN^2 monomers on them. Not more than one monomer could ever occupy a lattice site. All other sites were occupied by DMPC molecules which we henceforth ignored. We assumed that the process of polymerization proceeded very much more rapidly than any other time scale in the system. We shall return to this in the Discussion section. There are two other time scales: The characteristic time for a monomer to move through one lattice constant, which corresponds to ~0.9 nm, and the characteristic lifetime of excited radicals on the POMECY monomers. We took one MC step to represent

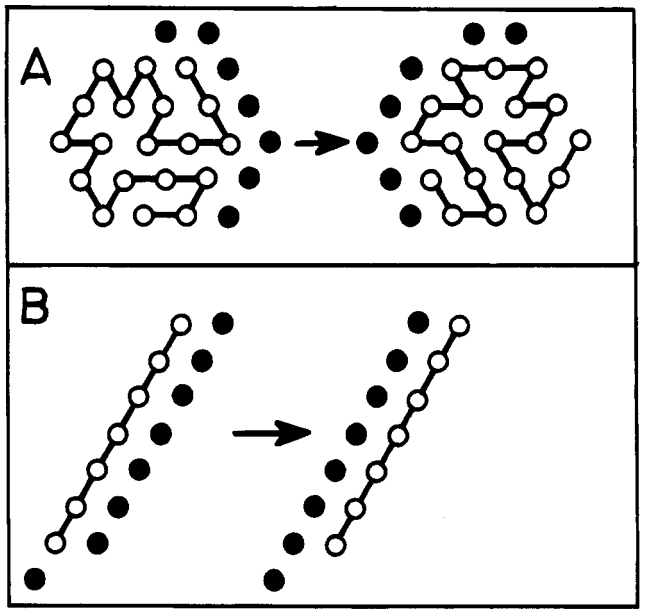

Figure 1. Movement of macrolipids in models II and III. (A) Model II. Hexagon translates to the right by one lattice constant and rotates by $\pi/3$ clockwise. (B) Model III. Rigid rod translates by one lattice constant.

the elapsed time of the former ($\sim 10^{-7}$ s), and we assigned a lifetime in units of MC steps. The polymerization, which takes place via the functional group attached to the polar group, is initiated by UV irradiation. The process of polymerization was modeled as follows:

(a) General Considerations. Each POMECY monomer, not part of a macrolipid ("free"), can be unexcited by the radiation (written as m) or free and excited (m*) or else part of a macrolipid (−m−, −m, or −m*), where a macrolipid is denoted by a sequence m−m−m− ··· −m−m or m*−m−m− ··· −m−m, the dashes indicating the chemical bonds. We did not permit polymers to become excited other than at their ends. Thus, states like m−m*−m− ··· −m−m, m−m−m*− ··· −m−m, etc., were not permitted. The implication of this is that we have excluded the modeling of polymer dissociation. This process, which is very interesting and becomes more important as the radiation intensity increases, was omitted because it would have involved yet another time scale. We shall comment, at the end, about the implications if this process is included.

(b) Excitation Procedure at Each MC Step. Irradiation was represented by choosing $N_I x N^2$ sites, occupied by monomers, randomly. If there was a free monomer at a chosen site, then it became excited in accordance with the rules of process a. If it was already excited, no change took place.

(c) Polymerization Procedure at Each MC Step. Each m* searched its nearest neighbors, and if these were m, m*, or −m*, it selected one of them randomly. A bond was then formed between the two monomers. In the first case the excitation (*) was passed to the m. In the other two cases, the excitations annihilated each other. Each −m* looked "ahead", in a direction opposite to the orientation of its bond or at the left and right neighbors of that site. If any of the three adjacent sites in those directions were occupied by an m, m*, or −m*, then one of them was chosen randomly. In performing this, the nearest-neighbor site ahead was given a weight w, while the two others were assigned weights of 1. The random choice was weighted by these quantities. The restrictions on the locations of the excitations were as described above (a and b). The choice of restricted relative bond angles was used because of the short intermolecular "spacers" in the POMECY polar group. By considering the structure of such molecules, it appears that, in order that the hydrocarbon chains be constrained to lie in the bilayer, the packing of these molecules must impose strong conditions on the general shape of macrolipids formed from them. We shall return to this point in the Discussion section. In each MC step, the polymerization procedure described here was attempted, carried out if allowed, and attempted again, and this was repeated until no excited monomer could form any further bonds. This procedure of attempting to polymerize as many monomers as possible before the monomers were again moved follows from our assumption that the polymerization takes place on a time scale faster than the monomer diffusion time scale. We shall comment on this in the Discussion section.

(d) Macrolipid Structure. All internal angles between two consecutive bonds on a macrolipid were constrained to be either π or $2\pi/3$. Bonds were created within this constraint and could not be created if it was violated.

(e) Excitation Lifetime. If a monomer had been an m* or an −m* for N successive MC steps, then at the $(N + 1)$st MC step a random number, R, was chosen, $0 \leq R < 1$. If $R > \exp(-N/N_L)$, then the monomer became deexcited. This procedure was carried out at every MC step with the appropriate values of N used for each excited monomer. The number N_L is the lifetime of an excited state in units of time appropriate to one MC step.

(f) Movement. At each MC step each unpolymerized monomer and each macrolipid attempted to translate by one lattice constant in a randomly chosen direction. The movement was allowed if it did not violate the constraint that not more than one monomer could occupy a lattice site. No attempt was made to rotate these macrolipids.

Computer Simulation. All simulations were carried out on lattices with periodic boundary conditions. We ran simulations on $(25)^2$ lattices, to model a DMPC−DPPC bilayer, averaging over 500 MC steps to confirm that the phase diagram which we obtained was the same as that measured and calculated before,[13] and to place the results for the various models of 4,16-POMECY within the context of a similar but nonpolymerized system. For model I, we used $(100)^2$ lattices and carried out averaging for 30 000 MC steps. Compared to the small lattices and short runs for DMPC−DPPC systems, such long runs are necessary because of the lengths of the polymers used. We studied polymers containing (degree of polymerization) 24, 48, and 88 monomers. For model II, we classified the hexagons according to "size": the number of concentric hexagons around the central site. If size is denoted by s, then the number of monomers is equal to $3s(s + 1) + 1$. We studied hexagons of sizes 1, 2, and 4. We used up to $(100)^2$ lattices and averaged up to 5000 MC steps. We did not need as many steps as in simulations of model I because the polymers are rigid and compact. For model III, we studied rigid rods containing up to 61 monomers, as to compare directly with the results of model II for $s = 4$. Because the linear extent of the rods is the degree of polymerization, we used lattices up to $(130)^2$ but required averaging only up to 1500 MC steps.

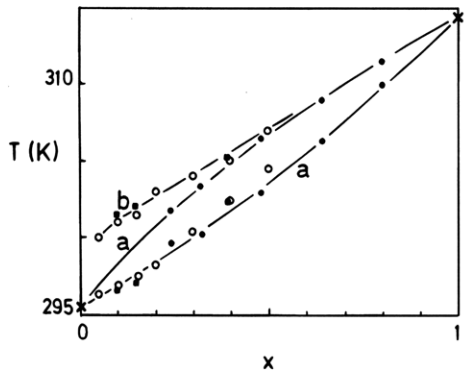

Figure 2. Calculated phase diagram of DMPC–DPPC bilayers (●, a) and DMPC–4,16-POMECY (model I; flexible self-avoiding single-length polymers) bilayers containing 24 (○) or 88 (■) monomers each (b). Phase transition temperatures of the pure systems are denoted by ×.

In order to be able to relate our phase diagrams to experiments, we calculated phase boundaries by analyzing the temperature dependence of the specific heat, C_p, at constant pressure. This is given by the derivative of the enthalpy with respect to T. We extrapolated the largest (absolute values of) slopes of C_p to the base line and used the temperatures obtained to identify the phase boundaries.

Finally, the simulations of the formation of macrolipids via the polymerization of POMECY monomers was done on $(200)^2$ lattices. Reliable statistics are now obtained, not by long runs, because we are dealing with a kinetic process which comes to an end, but by averaging over a sufficient number of similar simulations on sufficiently large lattices. By carrying out simulations on lattices of sizes ranging from $(100)^2$ to $(300)^2$, we found that the distributions obtained were unchanged for lattices of size $(200)^2$ and larger. We ran the simulations until 90% of the monomers had become polymerized. This required runs of up to $\sim 10^4$ MC steps, and we checked, by monitoring the approach to this limit, that the distributions of macrolipid lengths had achieved asymptotic values. We found that, as the monomer concentration, x, became larger, longer runs were needed to achieve 90% polymerization. We averaged distributions over 100 such simulations for each concentration of monomers.

All simulations were carried out on DEC3100, DEC5000/200, or IBM6000/320 or -350 workstations.

Results

We shall present the phase diagrams in terms of the concentration of POMECY monomers, x, and not mole percent POMECY macrolipids. This is so that we can compare our results with those of Eggl et al.[2] (Figure 3) where mole percent POMECY refers to the percentage of POMECY monomers.

Figure 2 (phase boundaries a) shows the calculated phase diagram for a DMPC–DPPC mixture, and it can be confirmed that it is essentially the same as that calculated before and which agreed with the experimental results.[13] In the same figure we show the calculated phase diagram for DMPC–4,16-POMECY bilayers using model I (phase boundaries b). Here, the macrolipids contain either 24 or 88 monomers, and it is clear that both cases exhibit essentially the same phase diagram (b). Figure 3 shows four typical instantaneous distributions for 24 monomers/macrolipid and different temperatures and concentrations. The results

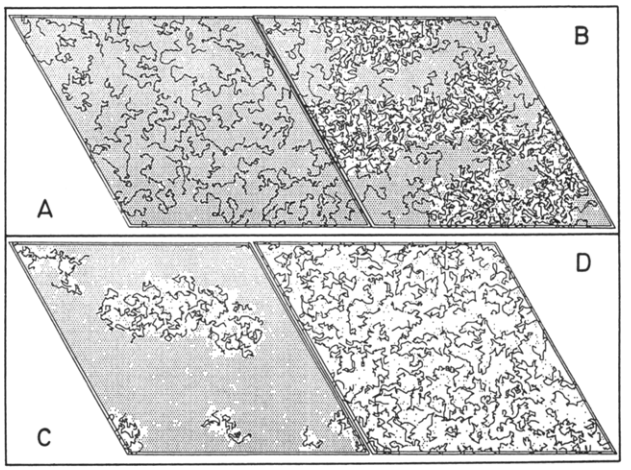

Figure 3. Instantaneous states of a DMPC–4,16-POMECY (model I; flexible self-avoiding single-length polymers) bilayer, for macrolipids containing 24 monomers. Dots indicate excited- or intermediate-state DMPC molecules, while blank areas indicate ground-state DMPC molecules. (A) $x = 0.2$, $T = 42.8$ °C. (B) $x = 0.4$, $T = 30.8$ °C. (C) $x = 0.1$, $T = 24.8$ °C. (D) $x = 0.3$, $T = 12.8$ °C.

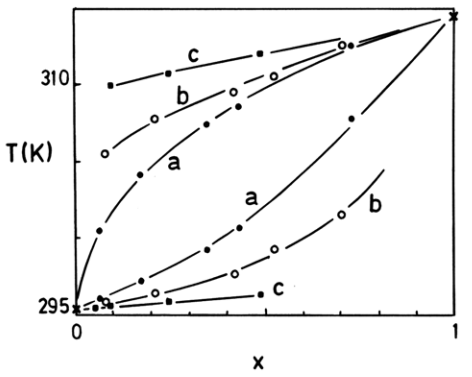

Figure 4. Calculated phase diagram of a bilayer of DMPC and 4,16-POMECY (model II; compact rigid single-size hexagons): size 1 (●, a), size 2 (○, b), and size 4 (■, c). Phase transition temperatures of the pure systems are indicated by ×.

for 88 monomers/macrolipid are essentially similar. By comparing Figures 2 and 3 we can see the two homogeneous phases (Figure 3, A and D) with the two-phase region at intermediate temperatures (Figure 3, B and C). Dots indicate excited- or intermediate-state DMPC molecules, while blank areas indicate ground-state DMPC molecules.

Figure 4 shows calculated phase diagrams for DMPC–4,16-POMECY using model II in which compact macrolipids are represented as hexagons. Shown here are the phase boundaries when the hexagons are of sizes 1 (a), 2 (b), and 4 (c). For the last named we did not go to monomer concentrations greater than ~50% since the behavior of the liquidus line was evident, and no solidus line was reported by Eggl et al.[2]

Figure 5 shows phase diagrams for DMPC–4,16-POMECY mixtures, using model III, in which the macrolipids are represented as rigid rods, one monomer in width, for degrees of polymerization 7, 19, and 61. These contain the same number of monomers as do hexagons of sizes 1, 2, and 4 (Figure 4). It can be seen that the two-phase regions are narrower in Figure 5 than the corresponding regions of Figure 4, when systems with the same number of monomers/macrolipid are compared.

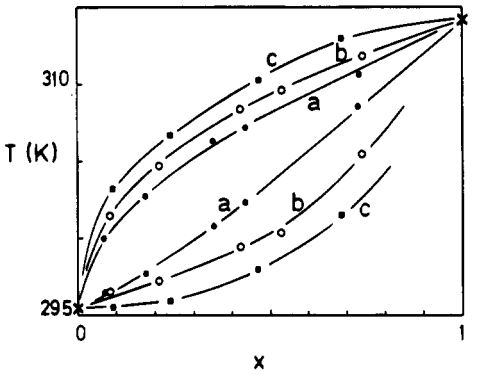

Figure 5. Calculated phase diagram of a bilayer of DMPC and 4,16-POMECY (model III; rigid single-length rods): rods with 7 monomers (●, a), with 19 monomers (○, b), and with 61 monomers (■, c). Phase transition temperatures of the pure systems are indicated by ×.

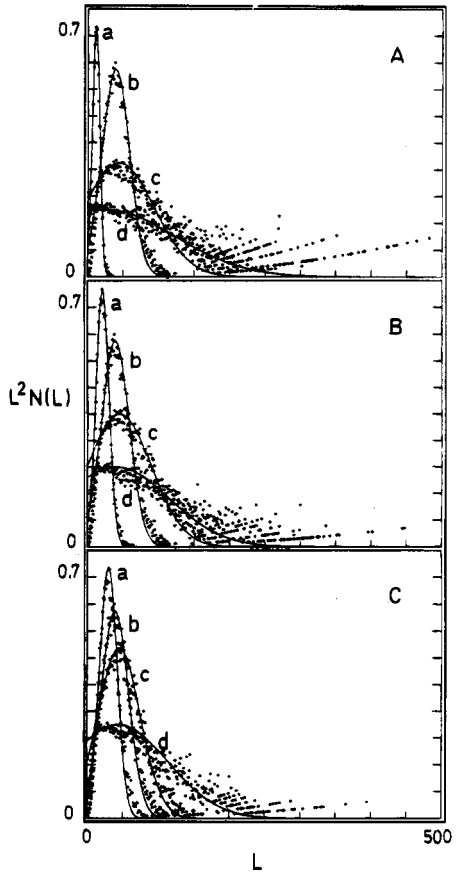

Figure 6. Unnormalized weight-averaged molecular weight distribution of macrolipids, formed by the polymerization procedure (see text), as a function of the degree of polymerization, for different monomer concentrations, x. (A) $x = 0.1$ (a), $x = 0.4$ (b), $x = 0.7$ (c), $x = 1.0$ (d). (B) $x = 0.2$ (a), $x = 0.4$ (b), $x = 0.6$ (c), $x = 0.9$ (d). (C) $x = 0.3$ (a), $x = 0.4$ (b), $x = 0.5$ (c), $x = 0.8$ (d). Gaussian curves fitted to the low-x distributions are to aid the eye.

Figure 6 shows distributions of the degree of polymerization as functions of monomer concentration. Shown here are $L^2N(L)$, the unnormalized weight-average molecular weight distribution, with $N(L)$ representing the fraction of polymers containing L monomers, as functions of L, the number of monomers per polymer, for monomer concentrations ranging from $x = 0.1$ to 1.0. For this simulation we had to chose an "intensity of UV irradiation", N_I, a relative weight, w, for polymerization to take place along the axis of the immediately preceding bond (i.e., ahead) compared to

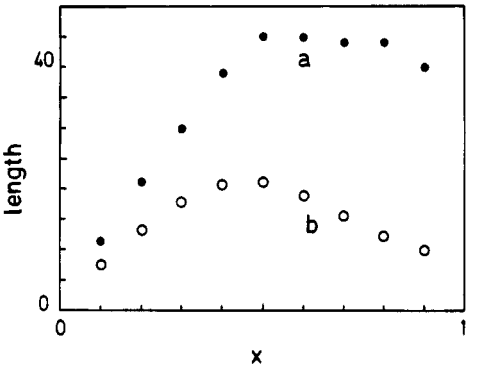

Figure 7. Most probable (●, a) and average (○, b) length of polymers formed by the polymerization process (see text) as a function of monomer concentration, x.

making an angle of $2\pi/3$ with the preceding bond, and a lifetime, N_L, of an excited monomer. These were all described above, but we shall discuss some general aspects of the POMECY macrolipid structure below. We chose $N_I = 2.5 \times 10^{-4}$, $w = 3$ (which gave a probability of 0.6 for forming a bond collinear with the preceding one in the macrolipid), and $N_L = 100$ MC steps (equivalent to $\sim 10^{-5}$ s). The last choice is in accord with the results of Meier et al.[16] regarding excited-state lifetimes. These choices were made in order that some long chains could form (small N_I) but with a sufficiently large N_I so that the simulation could be carried out in a reasonable time and with an excitation lifetime substantially longer than the "jump-time" (1 MC step) of monomers so that excited monomers could diffuse and thereby search for polymerizing opportunities. The results for $x = 0.4$ are shown on each graph in order to compare one graph with another. The low-L data for each concentration were fitted by Gaussian functions. The fit was adjusted by minimizing the mean-square deviation, excluding the high-L points. Such fits, however, are only used as an aid to the eye and to bring out the fact that the length distribution of polymers exhibits a low-L cluster, the peak of which changes as x changes, and a high-L tail. The results are shown in Figure 7 as functions of monomer concentration, where the average (excluding unpolymerized monomers) and most-probable lengths of macrolipids are shown. It can be seen that the most probable length increases essentially linearly with x until $x \approx 0.5$ and then remains very nearly constant. For the parameters that we chose, this maximum most probable length is ~40–45 monomers, but it is likely that this will depend upon the irradiation intensity represented by N_I.

Discussion

In the first part of the Theory section we outlined a model that enabled us to explain why monomeric 4,16-POMECY exhibits a phase transition at ~29 °C, some 12 °C below the corresponding transition in DPPC, the molecules of which also possess C-16 hydrocarbon chains, while 4,16-POMECY macrolipids, polymerized via their polar groups, exhibits a phase transition at ~45 °C, essentially in accord with its possession of two C-16 hydrocarbon chains. We ascribed the difference to the presence of a long polar group with a nonnegligible entropy when it is unpolymerized, proposing that the transition at 29 °C in monomeric 4,16-POMECY involves the "melting" not only of the hydrocarbon chains but also the polar group. When the polar group becomes polymerized, we propose that this entropy is

lost and the polar group will exhibit little change at the main hydrocarbon chain "melting" transition. Hence, polymerized 4,16-POMECY will "look like" DPPC, while unpolymerized 4,16-POMECY will possess the additional entropy of its polar group and exhibit a main transition some 12 °C below that of the macrolipids.

Because the polar groups have a cross-sectional area of two hydrocarbon chains available to one polar group chain, we have ignored the possibility of a substantial ordering of polar group chains. The kind of "melting" transition which we envisage in monomeric 4,16-POMECY involves the polar groups making transitions between states of moderate entropy and those of high entropy characteristic of "fluid" hydrocarbon chains. When they are polymerized, and thereby constrained, such a transition cannot occur.

We turn our attention, then, to bilayers of 4,16-POMECY and DMPC, and the phase diagram of this system (ref 2, Figure 3). The salient points of the experimental phase diagram of Eggl et al.[2] are clear: A linear increase of the liquidus line from ~24 to ~42 °C as x increases from 0 to ~0.4 and an essentially horizontal line between $x = 0.5$ and 0.9. The implication is that, for $x = 1.0$, pure polymeric 4,16-POMECY exhibits a phase transition at ~45 °C. The solidus line was not observed. A comparison of this phase diagram with those of Figures 2, 4, and 5 shows unambiguously that none of the latter are in accord with the experimental results. In particular, the model of 4,16-POMECY as a flexible self-avoiding chain (Figure 2) constrained to lie in two dimensions is, by far, the worst model. The closest model appears to be that of a compact rigid structure (Figure 4), but a liquidus line with a nearly-horizontal portion at high x involves far too steep an increase at low x (curve c).

There are at least two possibilities: One is that the POMECY macrolipids form nonplanar bilayer phases as x increases and, therefore, cannot be described by the models which we have used. Another is that these macrolipids are in locally-planar mixed lipid bilayers as we have described but that we have not taken into account an essential consideration. It is for that reason that we attempted to model the polymerization process itself.

We have presented results for one not-unrealistic model. Our intention is not to investigate all possible models of this process but to show that at least one acceptable model exhibits features which enable us to understand the experimental phase diagram. As described above, the important features of the model are the assumptions that polymerization can take place on a much shorter time scale than lipid lateral diffusion and that polymerization is anisotropic in that there is a higher probability of forming a bond collinear with the immediately preceding bond in the macrolipid. The other two features are true for this process:[2,3] the UV irradiation intensity is "low" and the lifetime of excited monomers is longer than the characteristic time for a monomer to move a distance equal to its cross-section diameter, in a fluid phase.

In order to consider the validity of our assumptions, we define τ_p to be the characteristic time for the polymerization of one additional monomer,

$$\mathrm{m{-}m{-}\cdots{-}m^* + m \rightarrow m{-}m{-}\cdots{-}m{-}m^*} \quad (15)$$

where the $-$m* and the m on the left side are nearest neighbors and are located so that polymerization can occur. We define τ_D to be the characteristic time for a lipid to diffuse over a distance equal to one monomer diameter and τ_L to be the lifetime of a monomer in a state excited by incident UV radiation. Our simulations have been carried out using the assumption that $\tau_p \ll \tau_D < \tau_L$. Various techniques yield values of phospholipid diffusion coefficients of $D \approx 10^{-7}$ cm^2/s.[14,15] If the diameter of the cross section of a lipid molecule, in a fluid phase, is ~9 Å, then the time, Δt, to move this distance is $\tau_D \approx 2 \times 10^{-8}$ s. Recently, Meier et al.[16] measured the lifetime, τ_L, of an excited monomer of the kind discussed here. They found that τ_L ranges from $\sim 10^{-7}$ to 3×10^{-7} s. Thus, τ_L is about 1 order of magnitude larger than τ_D. Finally, it is well-known that a polymerization process of the kind described here is diffusion-controlled and that the characteristic time, τ_p, is similar to that of excimer formation. This has recently been studied, and a characteristic time, $\tau_p \ll 10^{-8}$ s, was reported.[17]

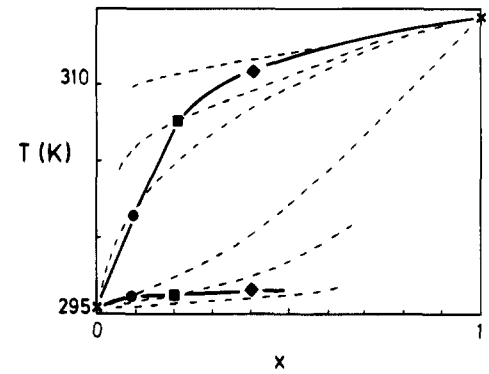

Figure 8. Phase diagram (symbols and solid lines) of a bilayer of DMPC and 4,16-POMECY (model II; compact rigid hexagons with sizes which depend upon monomer concentration, x, as in Figure 7a). Dashed lines are the phase boundaries for fixed-size hexagons (from Figure 4).

It is clear from the results summarized in Figure 7 that the most probable (as well as the average) length of polymerized macrolipids depends upon the monomer concentration x. Since the procedure employed in the experimental studies was to first make bilayers of DMPC and monomeric 4,16-POMECY of fixed x and then polymerize the latter,[2] the possibility that different concentrations of POMECY contain macrolipids of different average length must be taken into account.

Figure 8 shows a combination of the results of Figures 4 (model II, compact macrolipids) and 7. The position of the liquidus line now depends upon the length of the macrolipids, and we have chosen the most probable lengths. As x increases, we must use different phase boundaries calculated for fixed macrolipid lengths, and the true phase boundaries are the loci of these points. From Figure 7 the most probable lengths of 7 (size 1), 19 (size 2), and 37 (size 3) occur at $x \simeq 0.08$, $x \simeq 0.2$, and $x \simeq 0.4$, respectively, and these are plotted in Figure 8. We have interpolated the position of the phase boundaries for size 3 hexagons (filled diamond). A comparison of Figure 8 with Figure 3 of Eggl et al.[2] suggests that we have identified a possible explanation of the phase diagram of DMPC–4,16-POMECY bilayers.

Figure 9 shows a similar procedure carried out for the results of Figures 5 (model III, rigid rod macrolipids) and 7. The liquidus line does not exhibit the linear increase of Figure 8 at low x. However, it should be remembered that we did not allow the rigid rods to rotate in the simulation of model III so that the results of Figure 5 are for assumed nematic ordering of the macrolipids. It could be argued, though, that, as x

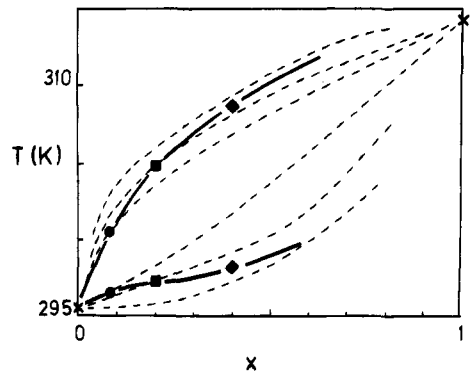

Figure 9. Phase diagram (symbols and solid lines) of a bilayer of DMPC and 4,16-POMECY (model III; rigid rods with lengths which depend upon monomer concentration, x, as in Figure 7a). Dashed lines are the phase boundaries for single-length rods (from Figure 5).

increases, the probabilities of occurrence of nonnematic distributions are small. For long rods of width one monomer, nonnematic packing might occur at low-x values.

The above considerations suggest that 4,16-POMECY macrolipids in lipid bilayers have an essentially rigid structure, either compact or composed of compact segments connected by rigid rods. Flexible models of this macrolipid appear to have phase diagrams not in accord with that deduced from light-scattering experiments.[2] The former conclusion is in accord with conclusions drawn from models of the lateral diffusion of tracer monomers in mixed DMPC–4,16-POMECY bilayers.[2] There only rigid compact structures or rigid rods were considered as models of 4,16-POMECY, and it was concluded that the macrolipids were combinations of both structures.

Our results are in agreement with what has been found, experimentally. Thus, when the UV radiation intensity (or initiator concentration) is very low, a few large polymers, and possibly only one, are formed which become segregated in the bilayer. When the initiator concentration is increased, then a broad distribution of smaller macrolipids is observed.[16] This, latter, effect is possibly due to the dissociation of macrolipids as well as to the creation of many excited monomers from which polymers may grow.

Large macrolipids can also dissociate into small macrolipids, even when the radiation intensity is low, if the irradiation is applied for a sufficiently long time. This is probably what has taken place in the macrolipid preparation carried out by Eggl,[2] who irradiated samples for ~10 min. Accordingly, it is likely that the distribution of macrolipid lengths obtained by Eggl is sufficiently correctly reflected in the distribution calculated, and made use of, by us.

A remaining question is whether our results, that 4,-16-POMECY macrolipids are essentially rigid, are in accord with what we known about the structure of the monomers. If we try to pack such monomers together in order to achieve short polar group bonds in the macrolipid polar region, then we find that linear polymers are preferred, with the polymer backbone connecting the monomers assuming a zigzag shape, when projected onto the plane of the bilayer. However, "defects" can form, which involve a change in average orientation of the polymer. This redirection of the polymerization process involves angular changes in the average backbone orientation of $\sim\pm\pi/3$. It is because of this that we chose the weighting factor, w (above), to be >1 so that such random reorientation can occur. The resulting polymers exhibit meanders and relatively compact regions connected by straight sections.

Conclusions

We have presented a model of 4,16-POMECY monomers and (polymerized) macrolipids in order to address three questions. The first is, why, with a pair of C-16 hydrocarbon chains, does the monomeric system exhibit a phase transition at $T_m^{up} \simeq 29$ °C? The second is, why, therefore, do the macrolipids exhibit a phase transition at $T_m^{p} \simeq 45$ °C? The third question is concerned with what the phase diagram, deduced by light-scattering experiments,[2] tells us about the macrolipid structure.

We conclude that an explanation of the first question is that the entropy of the relatively large polar group, which is about the same size as the hydrocarbon chains, can account for the decrease in T_m^{up} from ~41 °C (appropriate for C-16 chains) to the observed ~29 °C. When the macrolipids are formed via the polar groups, this entropy is lost and the transition therefore takes place at $T_m^{p} \approx 45$ °C. The slight difference between 41 and 45 °C might be due to a small change in the effective hydrocarbon chain lateral pressure (a possible increase by ~4 mN/m) or to slightly different chain–chain interactions. If this explanation is indeed correct, then there are two consequences:

(a) Some changes should be observed in the statics and dynamics of the monomeric 4,16-POMECY polar groups as the system undergoes the phase transition at $T_m^{up} \approx 29$ °C, and these changes should be essentially absent in polymerized 4,16-POMECY macrolipids.

(b) We can predict the approximate transition temperatures for 4,N-POMECY for $N = 14$ and $N = 18$. Recalling that "up" denotes unpolymerized (monomeric) POMECY and that p denotes polymerized macrolipids, we calculate that

$$T_m^{up}(4,14) \approx 15\ °C$$

$$T_m^{p}(4,14) \approx 28\ °C$$

$$T_m^{up}(4,18) \approx 44\ °C$$

$$T_m^{p}(4,18) \approx 59\ °C$$

By modeling the polymerization process under the assumption that $\tau_p \ll \tau_D < \tau_L$, where τ_p is the characteristic time for polymerization of a monomer (see above), τ_D is the monomer time scale for lateral diffusion over a distance of one monomer cross-section diameter, and τ_L is the lifetime of a monomer in a state excited by incident UV radiation, and excluding macrolipid dissociation, we found the following:

(c) The most probable length of the macrolipids increases linearly with monomer concentration, x, for $x < x_c$, after which it remains essentially constant for $x_c < x$.

(d) There is a distribution of many small macrolipids formed, from which the most probable length comes, and a broad distribution of very few, larger macrolipids.

By combining conclusion c with the results of the calculations of phase diagrams, we find that we can account for the phase diagram reported by Eggl et al.[2] and conclude the following.

(e) Polymerized 4,16-POMECY macrolipids in bilayers are probably rigid and compact, though possibly with rigid compact segments connected by rigid-rod-like segments.

We have predicted the position of the solidus line for mixed DMPC–4,16-POMECY bilayers.

Acknowledgment. This work was supported in part by grants from the Natural Sciences and Engineering Research Council of Canada (D.A.P.) and the Deutsche Forschungs Gemeinschaft (E.S.).

References and Notes

(1) Sackmann, E.; Eggl, P.; Fahn, C.; Bader, H.; Ringsdorf, H.; Schollmeier, M. *Ber. Bunsen-Ges. Phys. Chem.* **1985**, *89*, 1198.
(2) Eggl, P.; Pink, D.; Quinn, B.; Ringsdorf, H.; Sackmann, E. *Macromolecules* **1990**, *23*, 3472.
(3) Gaub, H.; Buschl, R.; Ringsdorf, H.; Sackmann, E. *Biophys. J.* **1984**, *45*, 725.
(4) Pink, D. A.; Green, T. J.; Chapman, D. *Biochemistry* **1980**, *19*, 349.
(5) Snyder, R. G.; Cameron, D. G.; Casal, H. L.; Compton, D. A. C.; Mantsch, H. H. *Biochim. Biophys. Acta* **1982**, *684*, 111.
(6) Corvera, E.; Laradji, M.; Zuckermann, M. *J. Phys. Rev. E* **1993**, *47*, 696.
(7) Doniach, S. *J. Chem. Phys.* **1978**, *68*, 4912.
(8) Pink, D. A. Theoretical Models of Monolayers, Bilayers and Biological Membranes. In *Biomembrane Structure and Function*; Chapman, D., Ed.; Macmillan Press: London, U.K., 1983.
(9) Pink, D. A. Computer Simulation of Biological Membranes. In *Molecular Description of Biological Membranes by Computer Aided Conformational Analysis*; Brasseur, R., Ed.; CRC Press: Boca Raton, FL, 1990.
(10) Metropolis, N.; Rosenbluth, A. W.; Rosenbluth, M. N.; Teller, A. N.; Teller, E. *J. Chem. Phys.* **1953**, *21*, 1087.
(11) Carmesin, I.; Kremer, K. *J. Phys. Fr.* **1990**, *51*, 915.
(12) Pink, D. A.; Merkel, R.; Quinn, B.; Sackmann, E.; Pencer, J. *Biochim. Biophys. Acta* **1993**, *1150*, 189.
(13) Caillé, A.; Pink, D. A.; deVerteuil, F.; Zuckermann, M. J. *Can. J. Phys.* **1980**, *58*, 581.
(14) Páli, T.; Horváth, L. I. *Biochim. Biophys. Acta* **1989**, *984*, 128.
(15) Köchy, T.; Bayerl, T. M. *Phys. Rev. E* **1993**, *47*, 2109 and references therein.
(16) Meier, H.; Sprenger, I.; Bärmann, M.; Sackmann, E. *Macromolecules*, in press.
(17) Merkel, R.; Sackmann, E. *J. Phys. Chem.* **1994**, *98*, 4428.

MA941104V